encit 2020

ABCM Associação Brasileira de Engenharia e Ciências Mecânicas

18th Brazilian Congress of Thermal Sciences and Engineering
November 16–20, 2020 (Online)

ENC-2020-0128
A SECOND LAW APPROACH FOR A PURE ETHANOL DROPLET INJECTION AND EVAPORATION IN A VARIABLE TEMPERATURE ENVIRONMENT - EFFECTS OF DIFFERENT EVAPORATION MODELS

A. J. T. B. de Lima
C. H. Rufino
F. A. F. Gomes
W. L. R. Gallo
Universidade Estadual de Campinas, Cidade Universitária "Zeferino Vaz", Faculdade de Engenharia Mecânica, 13093-970, Campinas, Brasil
alessandrojtblima@gmail.com, rufino119186@gmail.com, f.augustogomes@gmail.com, gallo@fem.unicamp.br

Abstract. *Droplet evaporation modeling is essential to predict how fuels evaporate before the beginning of the combustion process in internal combustion engines. Evaporation time and evaporation rate are some of the variables obtained through this model, which allows the calculation of the droplet heat-up process through time. The application of the second law of thermodynamics highlights the main sources of irreversibilities in specific processes. The purpose of this work is to show the main differences among some evaporation models known in the literature for a pure ethanol droplet injection and subsequently evaporation surrounded by typical in-cylinder gases during the compression phase of a spark-ignition (SI) engine. This study is developed under the view of the second law of thermodynamics, specifically through the calculation of entropy generation. Initially, the differences between droplet evaporation models are presented, with special focus given to the heat-up process. Later, the differences among these models are highlighted for different air-fuel ratio conditions in terms of evaporation time, droplet penetration inside the cylinder gas, entropy generation, and evaporative cooling effect, indicating details related to fuel different injection moments during a SI engine cycle.*

Keywords: *second-law of thermodynamics, droplet evaporation, ethanol, direct injection*

1. INTRODUCTION

Currently, global environmental issues require a continuous enhancement of efficiency among all energetic processes. The efficiency of combustion processes relies on adequate fuel atomization. For direct injection of fuel, the spray depends on several droplet breakup regimes (Elkotb, 1982). Thus, droplet evaporation is directly related to fuel injection, belonging to spray injection and combustion processes (Lefebvre, 2017). Literature provides several classic reviews in droplet evaporation (Faeth, 1977), (Sirignano, 1983), which provides fundamental information related to this phenomenon. More recent reviews also present the fundamentals and update the knowledge regarding droplet evaporation at the current state of art (Sazhin, 2006), (Sazhin, 2017).

Droplet evaporation modeling allows different levels of mathematical assumptions regarding its solution. Some authors describe six different levels of computational modeling related to this subject (Sirignano, 2010), (Sazhin, 2014). Thermal conduction limit and convection approaches take into account not only the interaction between a quiescent environment with the droplet but also the relative velocity between them, affecting both Nusselt and Sherwood number correlations (Sirignano and Law, 1978), (Aggarwal and Peng, 1995).

The application of the second law of thermodynamics provides detailed information related to availability losses associated with thermodynamic processes (Bejan, 2006). This methodology has already been applied to internal combustion engines (ICEs), regarding combustion, gas exchange, and turbocharging processes, as presented by Rakopoulos and Giakoumis (2006). Second law analyses related with droplet evaporation and combustion exist in the literature (Sengupta, 1987), (Som *et al.*, 1990), (Dash and Som, 1991), even though there are not many details regarding this method on this specific phenomenon, with very scarce reviews available in the literature (Som and Datta, 2008).

Therefore, the purpose of this work is to show the main differences among four influential evaporation models known in the literature for a pure ethanol droplet on the processes of injection and evaporation in typical in-cylinder gases during the compression phase of a spark-ignition engine under a second law of thermodynamics view. First, the main differences between droplet evaporation models are highlighted regarding the heat-up process in a base-case simulation. The evaporation models are subsequently used for simulating the evaporation process of a single droplet injected in an environment similar to the in-cylinder gases during a compression stroke. Mass, momentum, energy, and entropy

balances are solved for the droplet while mass, energy, and entropy balances are solved for the environment under rich, stoichiometric, and lean air-fuel ratio conditions. The results expose the differences between four evaporation models in terms of evaporation time, droplet penetration inside the cylinder gas, entropy generation, and evaporative cooling effect, in addition to reveal details regarding specific periods of direct injection of fuel in an ICE.

2. METHODOLOGY

2.1 Model description and assumptions

The model involves the injection of a pure ethanol droplet inside a system with air simulating an internal combustion engine operation during the compression stroke. This particle begins to evaporate at the moment it is injected into this system, as the gases are at a higher temperature than the droplet. Both temperature and ethanol concentration gradients exist in the interface between the droplet surface and the gas environment. There is a relative velocity between the particle and the gas, which is at rest. This relative velocity stimulates the convective heat and mass exchange between the droplet surface and the air. The Ranz-Marshall correlation was used to calculate both Nusselt and Sherwood numbers (Ranz and Marshall Jr., 1952). The simulation is executed until the droplet reaches a diameter of approximately $2\mu m$, respecting the continuum assumption. Two control volumes are applied in this study: first, the control volume that involves the droplet and follows the droplet diameter reduction; thus, it has a variable volume. Second, the control volume that represents the surrounding gas, whose volume is also variable. The junction of these control volumes represents the engine cylinder, whose volume is considered constant over time.

In order to make this model feasible, the authors apply the following hypotheses. It is considered that the evaporation process is quasi-steady. Also, the liquid density is uniform throughout the droplet. Thermodynamic, thermophysical and mass diffusivity properties are constant at each time step, despite variations occur between different time steps. The initial surrounding gas composition is dry air. Soret and Dufour effects are ignored. There is no shaft or viscous work on control surfaces. There is also no droplet rotation and non-inertial effects on this model. Thermal radiation, chemical reactions, and potential energy are considered negligible on this model. The control volume which involves the air is adiabatic and rigid on all its surfaces, with exception of its interface with the particle. The surrounding air is insoluble in liquid anhydrous ethanol. The droplet temperature is uniform through its volume. The one-third rule is used to calculate the mixture properties (Abramzon and Sirignano, 1989). The droplet is the only condensed phase and attains its spherical shape during the evaporation process and there is no interaction between different droplets. The thermodynamic properties used in the model (enthalpy, entropy, free Gibbs energy) are obtained based on NIST thermodynamic tables (Chase Jr., 1998). Liquid ethanol properties are calculated based on correlations from (Green and Perry, 2008). Gas properties are calculated utilizing the open-source software Cantera.

2.2 Droplet modeling

The authors applied the conservation laws (mass, momentum, and energy) and entropy balance on their integral forms to obtain equations to the droplet, whereas only mass, energy, and entropy equations were applied to the gas, as the authors consider that the gas is quiescent (Kuo, 2005). Based on (Abramzon and Sirignano, 1989), (Crowe *et al.*, 2012) and (Pinheiro, 2018), the equation set for the droplet is presented by Eqs. (1-5):

$$\frac{\mathrm{d}m_d}{\mathrm{d}t} = -\dot{m} \tag{1}$$

$$\dot{m} = \pi D_d \rho_m D_m Sh_m ln(1 + B_M) \tag{2}$$

$$\frac{\mathrm{d}D_d}{\mathrm{d}t} = -\frac{2\dot{m}}{\pi \rho_d D_d^2} \tag{3}$$

$$\frac{\mathrm{d}u_d}{\mathrm{d}t} = \frac{3}{4}\frac{C_d}{D_d}\frac{\rho_m}{\rho_d}|u_g - u_d|(u_g - u_d) \tag{4}$$

$$\frac{\mathrm{d}T_d}{\mathrm{d}t} = \frac{\pi D_d^2 h_{conv}(T_g - T_d) - \dot{m}\Delta h_v}{m_d c_d} \tag{5}$$

Where m_d is the droplet mass, $\dot{m}$ is the evaporation mass flow rate, D_d is the droplet diameter, ρ_m is the mixture density between droplet gas interface and surrounding gas. D_m is the mixture mass diffusivity, Sh_m is the mixture

Sherwood number, B_M is the mass transfer Spalding number. For the droplet velocity equation, u_d is the droplet velocity, u_g is the gas velocity, C_d is the drag coefficient whose value is obtained by the correlation presented in (Abramzon and Sirignano, 1989). For the droplet energy equation, T_d is the droplet temperature, h_{conv} is the heat transfer convective coefficient, Δh_v is the heat of vaporization for ethanol, c_d is the specific heat of ethanol.

The evaporation rate presented in Eq. (2) is adjusted based on which evaporation sub-model is applied, just as presented in (Pinheiro, 2018) and (Abramzon and Sirignano, 1989).

The entropy equation for the droplet showed to be linearly dependent with the energy equation, therefore it presents that the evaporation at a uniform temperature is a reversible process. Thus, we do not present the droplet entropy equation here.

2.3 Surrounding gas modeling

The Reynolds Transport Theorem equations are also applied to the surrounding gas to obtain the mass, equation, and entropy relations to this control volume. Equations (6-11) present these expressions:

$$\frac{\mathrm{d}m_{CV2}}{\mathrm{d}t} = \dot{m} \tag{6}$$

$$\frac{\mathrm{d}\rho_g}{\mathrm{d}t} = \frac{\pi D_d^2}{(V_t - \frac{1}{6}\pi D_d^3)} \frac{(\rho_g - \rho_d)}{2} \frac{\mathrm{d}D_d}{\mathrm{d}t} \tag{7}$$

$$\frac{\mathrm{d}T_g}{\mathrm{d}t} = \frac{\dot{m}\left(h_v - u_g + \frac{u_d^2}{2}\right) - \pi D_d^2 h_{conv}(T_g - T_d) + \frac{\pi}{2} D_d^2 p_g \frac{\mathrm{d}D_d}{\mathrm{d}t}}{(m_t - m_d)c_{p,g}} \tag{8}$$

$$\dot{\sigma}_{CV2} = \dot{m}(s_g - s_v) + (m_t - m_d)\frac{\mathrm{d}s_g}{\mathrm{d}t} + \pi D_d^2 h_{conv}\frac{T_g - T_d}{T_d} \tag{9}$$

$$\frac{\mathrm{d}s_g}{\mathrm{d}t} = \frac{c_{p,g}}{T_d}\frac{\mathrm{d}T_d}{\mathrm{d}t} - \frac{R_u}{W_g p_g}\frac{\mathrm{d}p_g}{\mathrm{d}t} - g_v\frac{\mathrm{d}n_v}{\mathrm{d}t} \tag{10}$$

$$\frac{\mathrm{d}p_g}{\mathrm{d}t} = \frac{R_u}{W_g}\left(\rho_g\frac{\mathrm{d}T_g}{\mathrm{d}t} + T_g\frac{\mathrm{d}\rho_g}{\mathrm{d}t}\right) \tag{11}$$

Where m_{CV2} is the surrounding gas mass, m_t is the total mass and V_t is the cylinder volume. For the gas energy equation, T_g is the gas temperature, h_v is the ethanol gas enthalpy, u_g is the gas internal energy and $c_{p,g}$ is the gas constant-pressure specific heat. For gas entropy equation, $\dot{\sigma}_{CV2}$ is the entropy generation from control volume 2, s_g is the gas entropy, s_v is the ethanol gas entropy, R_u is the universal gas constant, W_g is the gas molar mass, p_g is the gas pressure, g_v is the vaporized ethanol Gibbs free energy and n_v is the ethanol vapor number of moles.

2.4 Droplet evaporation sub-models

There are four evaporation sub-models analyzed in this work: the classical evaporation model (CEM), the modified classical evaporation model, the non-equilibrium model, and the Abramzon and Sirignano model. The first model uses all equations presented previously. The modified classical model applies a correction factor G, described by Eqs. (12-13) in (Pinheiro, 2018).

$$G = \frac{\beta}{e^{\beta} - 1} \tag{12}$$

$$\beta = -\frac{\dot{m}c_{p,m}}{2\pi k_m D_d} \tag{13}$$

Where β is a non-dimensional evaporation parameter and k_m is the mixture thermal conductivity.

The non-equilibrium model presented in (Pinheiro, 2018) assumes a non-equilibrium behavior on vapor molar fraction, hence a deviation term is added to the calculation. Finally, Abramzon and Sirignano model (Abramzon and Sirignano, 1989) incorporates the film theory to calculate correction factors for the thickness of thermal and diffusional films.

2.5 Solution method

In order to solve the system of equations and investigate the droplet evaporation, a 4th Runge-Kutta ordinary differential equation (ODE) solver was implemented.

3. RESULTS AND DISCUSSION

3.1 Base-case analysis

The result section first presents a base-case simulation for the previously described evaporation model. The intention is to highlight the main differences in the outputs obtained from the four models. The initial conditions are $D_d = 25\mu m$, $T_d = 288.15K$, $u_d = 10m/s$, $T_g = 900K$, $p_g = 1823.85kPa$ (18 atmospheres). Figure 1 shows the droplet and surrounding gas temperatures over time. The classical approach is taken into account for this case with a stoichiometric air-fuel ratio. The droplet temperature increases rapidly and near 0.3ms reaches a peak value. Additionally, the classical model predicts a slight cooling of droplet temperature after its peak, indicating that the evaporation process removes more energy from the droplet than the convection heat transfer provides to it. Moreover, the final temperature is near the wet-bulb temperature for ethanol under the final gas condition. On the other hand, the gas temperature monotonically decreases during the process (almost 125K). This result highlights the beneficial effect of evaporative cooling on the gas. Under conditions of a finite environment, the evaporation time increases when compared to an infinite environment, since the gas cooling over time affects negatively the convection phenomenon, hence it slows down the evaporation process on more realistic conditions.

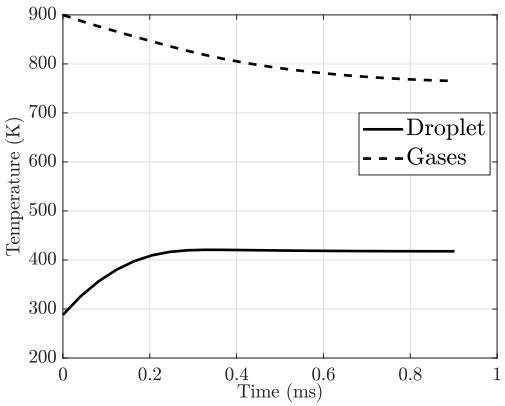

Figure 1. Droplet and surrounding gas temperatures over time. (base-case + classical model)

Another result that corroborates the different behavior of this analysis is presented by Fig. 2, where the gas pressure profile is presented over time. The pressure notably reduces from 1800 to near 1600 kPa, therefore it interferes with the evaporation process by the vapor mass fractions over the droplet surface and the average mass fractions in the gas. The pressure reduction is justified by the gas cooling effect and by its control volume increase, as the droplet evaporates over time. Another information available in the figure is the partial pressure of ethanol over time. Its behavior is similar to the droplet temperature, but it highlights the soft reduction after its peak. Under the final conditions of pressure and temperature, the ideal gas validity for ethanol is checked by calculating the compressibility factor, which is near 0.90, which indicates that, for this case, the ideal gas model for ethanol is at its limit of validity.

Figures 3 (a) and (b) present the droplet and surrounding gas temperature profiles over time for all four evaporation models mentioned in this paper. The time is normalized to compare the temperatures on the same basis. In the sub-figure 3 (a), it is evident that the classical model indicates the highest temperatures after the initial phase of evaporation. Additionally, it does not decelerate near 0.05, as it happens with the other three models. Therefore, the classical model overestimates the amount of energy transferred from the gases to the droplet. Another interesting characteristic of the left figure is that the temperatures of modified classical and non-equilibrium models do not tend asymptotically after the early moments of evaporation. These two models reach almost the same value during the whole simulation and reach the same value as the Abramzon model in the end. This last model's temperature profile presents an intermediate behavior, among overestimated classical and the other two models. In the sub-figure 3 (b), the classical model underestimates the gas temperature cooling effect, although the difference among its result and the other three models is not significant (near 4K) at the end. Moreover, the other three models present the same profile for the gas temperature.

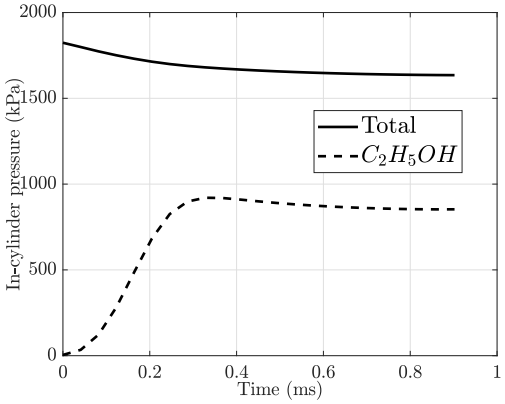

Figure 2. Surrounding gas pressure over time. (base-case + classical model)

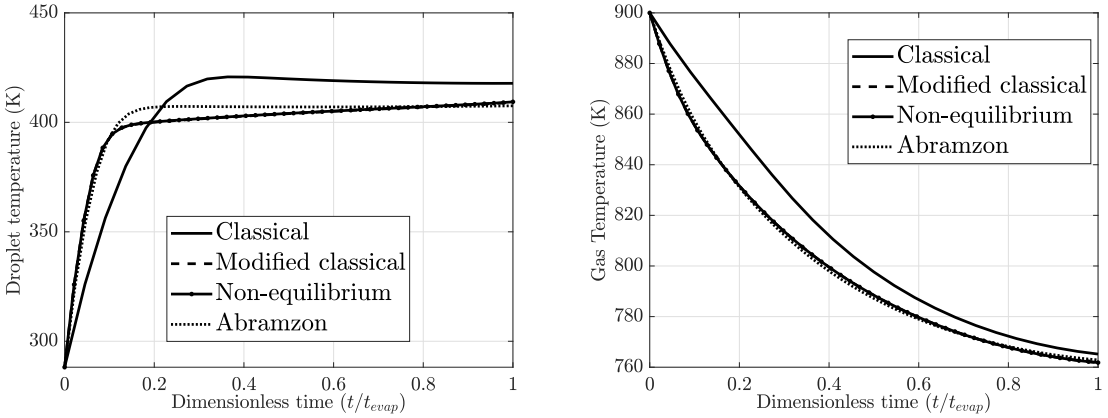

Figure 3. Left (a): Droplet temperature profile; right (b): the surrounding gas temperature profile for different evaporation models - base-case.

The final result for the base-case analysis is the droplet diameter variation over dimensionless time, which is shown by Fig. 4. On the same time basis, the classical model overestimates the diameter during the whole process, instead of the other three models, which follow similar profiles. Moreover, the relative difference between the diameters may reach the maximum value of 10% in 0.35 dimensionless time, therefore they directly yield different results regarding the droplet surface for heat transfer, for instance.

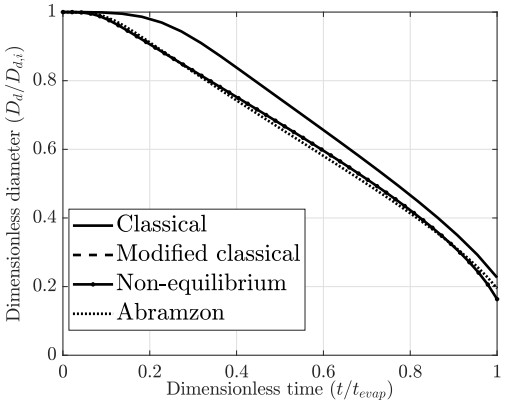

Figure 4. Droplet diameter profiles for different evaporation models - base-case.

3.2 Relative air-fuel ratio effects on droplet evaporation

This section shows the main effects of applying different relative air-fuel ratios in the air-fuel mixture on the evaporation process of a fuel droplet during the compression phase of a SI engine. The results related to the droplet are presented

in terms of its lifetime and penetration, while for the surrounding gas are presented the evaporative cooling effect and the entropy generation. Additionally, these results highlight the main differences found for the four mentioned models in terms of these four variables.

First, droplet evaporation time and air-fuel ratio are shown in Fig. 5 for a state representing the final compression phase of an ordinary spark-ignition engine (the base-case). The evaporation time decreases as the air-fuel ratio increases for all four models. The reduction is near 20% from the richest to the leanest mixture. The amount of surrounding gas over the droplet affects the evaporation process, since the higher the amount of mass the lower is the evaporative cooling effect over the gas temperature. Therefore, the time required to evaporate completely the droplet increases at richer air-fuel ratios. Furthermore, the classical evaporation model clearly underestimates the droplet lifetime, while the three others estimate higher times. The modified classical and non-equilibrium models predicted similar results in almost all cases presented here. Finally, the consolidated Abramzon model (Abramzon and Sirignano, 1989) predicted an intermediate result, although more closely to the modified classical and non-equilibrium than to the classical model.

Independently of the chosen model, the order of magnitude of time shown for this condition is approximately $10°$of crank angle (for an engine with 1000 RPM engine speed). This value indicates how long it would take for a droplet to evaporate inside the cylinder under these conditions, which corresponds to a realistic condition for a droplet fuel in direct-injection spark-ignition (DISI) engines.

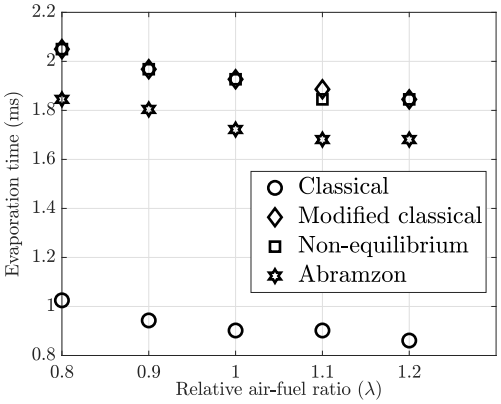

Figure 5. Evaporation time versus ethanol air-fuel ratio for different evaporation models.

Figure 6 presents the droplet penetration on different relative air-fuel ratios for all four models. Droplet penetration is slightly reduced with higher relative air-fuel ratios since the droplet lifetime and pressure drop reduces on leaner mixtures. Moreover, the model which deviates clearly from all results is the classical model, underestimating the droplet displacement. This behavior is related to the underestimation of evaporation time. Meanwhile, the other three models agree well on all conditions.

The utility of droplet penetration is to identify a possible occurrence of fuel impingement on cylinder walls, which cause unburned fuel emissions in ICEs. Based on the presented results, it is unlikely to occur such phenomenon on the conditions presented here, since the values are too low for an ordinary cylinder bore or stroke on automotive engines, for instance.

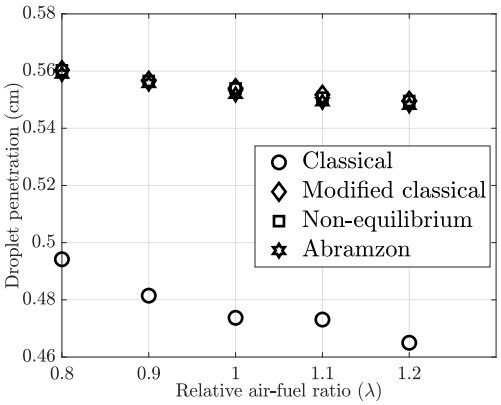

Figure 6. Droplet penetration versus ethanol air-fuel ratio for different evaporation models.

The evaporative cooling effect caused by droplet evaporation in the surrounding gases on different relative air-fuel

ratios is shown by Fig. 7. Richer relative air-fuel ratios cause higher temperature reductions in the surrounding gas, as the amount of air available to provide enough energy to cause evaporation is reduced. The difference between the extremes ($\lambda = 0.8$ and $\lambda = 1.2$) reaches almost 50K for all mentioned models. Furthermore, the four evaporation models did not present great differences in this result, although the classical model underestimates a little the gas cooling in all cases.

The benefit of evaporation cooling in DISI engines is to reduce the gas temperature before fuel combustion starts, which may avoid the occurrence of knock phenomenon under specific conditions in the engine. Therefore, this extra cooling effect obtained from fuel direct injection during the compression phase offers a possible perspective of a compression ratio increase and extra power per engine cycle.

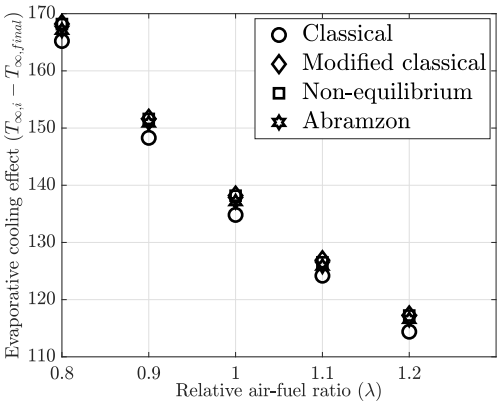

Figure 7. Gas evaporative cooling versus ethanol air-fuel ratio for different evaporation models.

Figure 8 shows the entropy generation occurred in the surrounding gas control volume for all evaporation models. The classical evaporation model indicates the lowest entropy generation for all cases, independently of the air-fuel ratio. This result connects directly with underestimated droplet evaporation times and overestimated convection effects on the droplet surface. Therefore, the classical model reflects an ideal condition in which evaporation does not occur. The other models present a higher entropy generation, which indicates more realistic calculations in terms of time evaporation and second law effects. The Abramzon model, which takes into account the film theory, yields an intermediate result both in terms of evaporation time and entropy generation among the four models. Another point to be considered is the main source of irreversibility on this process, which is the convective heat transfer, with minor contributions from the fuel-gas mixture. Furthermore, the leaner conditions showed the lowest specific entropy generation, followed by the stoichiometric and at last the richer conditions. This behavior is connected with lower gas temperature reduction and droplet lifetime found in leaner conditions, which suggests a more efficient evaporation process.

The obtained results for entropy generation offer the possibility of a thermodynamic optimization together with the main common evaporation variables such as those presented in this study, i.e., droplet lifetime and penetration. A connection between these variables is evident. Thus, lower entropy generation presents a possibility to offer optimal conditions to fuel direct injection in engines during the compression phase.

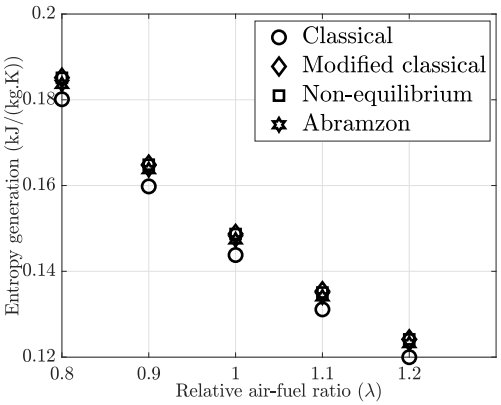

Figure 8. Surrounding gas entropy generation versus ethanol air-fuel ratio for different evaporation models.

4. CONCLUSION

This paper focuses on presenting the main differences related to four droplet evaporation models known in the literature for a pure ethanol droplet injection and subsequently evaporation in typical in-cylinder gases during the compression phase of a spark-ignition engine. A set of ordinary differential equations is provided for the droplet and finite surrounding gas with special attention to evaporation effects on gases via the second law of thermodynamics. A series of different conditions for the cylinder gas are covered with the air-fuel ratio on the view of four different droplet evaporation models presented in the literature.

Differently from consolidated droplet evaporation analyses existent in the literature, the presented droplet temperature profile has a slight reduction after the temperature peak and a high reduction in gas temperature, which is an indication of the evaporative cooling effect on the surrounding gas. This cooling can be used to prevent the knock effect during the combustion phase in a spark-ignition engine with ethanol direct injection.

The obtained evaporation times and droplet penetration are reduced at leaner relative air-fuel ratios. This result suggests possible adjustments at direct injection timing during the compression phase in order to reach a more efficient evaporation process.

The main differences between the four different evaporation models are highlighted. Special attention must be given to the classical model, whose temperature overestimates the evaporation effect, besides it differs from the other three models in most presented cases. On the other hand, the Abramzon model presents a intermediate behavior regarding droplet lifetime and entropy generation. Additionally, this model yields more realistic results than the other three models, since it is the only one who takes into account the film effects in the phenomenon, therefore it seems to be the most reliable evaporation model.

Lastly, the analysis indicates a higher specific entropy generation in the surrounding gas for richer air-fuel ratio conditions than on leaner ones. This behavior opens the possibility to a future work of thermodynamic optimization of the droplet evaporation process on lean conditions (partial load), which could offer interesting conditions of droplet lifetime, penetration, and evaporative cooling effect on specific fuel direct injection moments, therefore enhancing the first and second law efficiencies of this part of the engine cycle.

5. ACKNOWLEDGEMENTS

The authors would like to express their gratitude to “Conselho Nacional de Desenvolvimento Científico e Tecnológico (CNPq)” for the financial support through the process number 168894/2018-1.

6. REFERENCES

Abramzon, B. and Sirignano, W.A., 1989. “Droplet vaporization model for spray combustion calculations”. *International Journal of Heat and Mass Transfer*, Vol. 32, No. 9, pp. 1605–1618.

Aggarwal, S.K. and Peng, F., 1995. “A Review of Droplet Dynamics and Vaporization Modeling for Engineering Calculations”. *Journal of Engineering for Gas Turbines and Power*, Vol. 117, No. 3, pp. 453–461.

Bejan, A., 2006. *Advanced Engineering Thermodynamics*. John Wiley and Sons, 3rd edition.

Chase Jr., M.W., 1998. “NIST-JANAF Thermochemical Tables”. *American Chemical Society; American Institute of Physics for the National Institute of Standards and Technology*.

Crowe, C.T., Schwarzkopf, J.D., Sommerfeld, M. and Tsuji, Y., 2012. *Multiphase Flows with Droplets and Particles*. CRC Press, 2nd edition.

Dash, S.K. and Som, S.K., 1991. “Transport processes and associated irreversibilities in droplet combustion in a convective medium”. *International Journal of Energy Research*, Vol. 15, No. 7, pp. 603–619.

Elkotb, M.M., 1982. “Fuel atomization for spray modelling”. *Progress in Energy and Combustion Science*, Vol. 8, No. 1, pp. 61–91.

Faeth, G.M., 1977. “Current status of droplet and liquid combustion”. *Progress in Energy and Combustion Science*, Vol. 3, No. 4, pp. 191–224.

Green, D.W. and Perry, R.H., 2008. *Perry’s Chemical Engineers Handbook*. Mc-Graw Hill, 8th edition.

Kuo, K.K., 2005. *Principles of Combustion*. John Wiley and Sons, 2nd edition.

Lefebvre, A.H., 2017. *Atomization and Sprays*. CRC Press, 2nd edition.

Pinheiro, A.P., 2018. *Lagrangian modeling of droplet evaporation*. Ph.D. thesis, Universidade Federal de Uberlândia, Uberlândia, Brasil.

Rakopoulos, C.D. and Giakoumis, E.G., 2006. “Second-law analyses applied to internal combustion engines operation”. *Progress in Energy and Combustion Science*, Vol. 32, No. 1, pp. 2–47.

Ranz, W.E. and Marshall Jr., W.R., 1952. “Evaporation from Drops”. *Chemical Engineering Process*, Vol. 48, No. 3, pp. 141–146.

Sazhin, S.S., 2006. “Advanced models of fuel droplet heating and evaporation”. *Progress in Energy and Combustion*

Science, Vol. 32, No. 2, pp. 162–214.

Sazhin, S.S., 2014. *Droplets and Sprays*, Vol. 9781447163. Springer London, 1st edition.

Sazhin, S.S., 2017. "Modelling of fuel droplet heating and evaporation: Recent results and unsolved problems". *Fuel*, Vol. 196, pp. 69–101.

Sengupta, S.P., 1987. "Theorical studies on some aspects of droplet and spray evaporation". Technical report, IIT - Kharagpur.

Sirignano, W.A., 1983. "Fuel droplet vaporization and spray combustion theory". *Progress in Energy and Combustion Science*, Vol. 9, No. 4, pp. 291–322.

Sirignano, W.A., 2010. *Fluid Dynamics and Transport of Droplets and Sprays*. Cambridge University Press, 2nd edition.

Sirignano, W.A. and Law, C.K., 1978. "Transient Heating and Liquid-Phase Mass Diffusion in Fuel Droplet Vaporization". *Combustion and Flame*, Vol. 12, pp. 3–26.

Som, S.K. and Datta, A., 2008. "Thermodynamic irreversibilities and exergy balance in combustion processes". *Progress in Energy and Combustion Science*, Vol. 34, No. 3, pp. 351–376.

Som, S.K., Mitra, A.K. and Sengupta, S.P., 1990. "Second Law Analysis of Spray Evaporation". *Journal of Energy Resources Technology*, Vol. 112, No. 2, pp. 130–135.

7. RESPONSIBILITY NOTICE

The authors are solely responsible for the printed material included in this paper.